Abstract No. Vett0461

Dislocation Loops Formed During the Degradation of Forward-Biased 4H-SiC p-n Junctions

W. M. Vetter, M. Dudley (SUNY at Stony Brook), J. Q. Liu, M. Skowronski (Carnegie Mellon Univ.), H. Lendenmann (Linköping University) and C. Hallin (ABB Group Services Center)

Beamline: X19C

Introduction: A type of structural defect has been observed to develop in the epilayer portion of hexagonal silicon carbide diodes during their operation under forward carrier injection. The growth of the defect correlates with a degradation of electrical performance, an increase in the forward voltage drop [1]. The bounding partial dislocations were first observed by electroluminescence and then called "bright-line defects" [2]. It was possible to observe short lengths of the stacking fault's bounding partials by high-resolution transmission electron microscopy and determine that they were of the Shockley type with Burgers vector $\frac{1}{3}<10\bar{1}0>$ [3], but, as the field of view in electron microscopy is limited, the nature of the bounding partials was not explored about the whole circumference of a stacking fault.

Methods and Materials: 4H-SiC diodes were fabricated on 300 μm n-type wafers (n = 8 x 10^{18} cm^{-3}) as described in [4]. The thickness of the n^- layer in the diode structure was between 30 and 40 μm while the electron concentration was below 10^{15} cm^{-3}. The top of the structure was a p^+ epilayer. The area of the diode was 1×1 mm. Prior to x-ray topography, the contact layers on the surfaces of the diode were removed by etching in 10% hydrofluoric acid. The sample was then thinned from its back side to a thickness of 80 μm by mechanical polishing, then finished with 0.25 μm diamond paste. Synchrotron white-beam topographs were recorded in the transmission geometry and in the back-reflection geometry.

Results: Synchrotron white-beam topographs of diodes which had undergone stressing, taken in the transmission geometry, showed stacking faults which ranged in size between 15 and 500 μm across. They had either the triangular or parallelogram shapes such as have been previously reported. in figure 1. A rhomb-shaped stacking fault bordered by partial dislocation lines is labeled **R** in figure 1. This stacking fault's contrast is seen at its maximum in the topograph in 1(a), where **g** = $0\bar{1}10$. The fault contrast is visible in topographs taken with $(10\bar{1}0)$ reflections such as in figure 1(a), but is absent in $(11\bar{2}0)$ topographs such as figure 1(b), whose g-vector is $11\bar{2}0$. This behavior is consistent with a stacking fault that lies on the basal plane, because, while there is a phase shift associated with diffraction by the $(10\bar{1}0)$ reflections of a hexagonal crystal, there is none with the $(11\bar{2}0)$ reflections. The dislocation lines that border the stacking fault appear in all $(10\bar{1}0)$ reflections, and are apparent in the $11\bar{2}0$ reflection in figure 1(b). In the $2\bar{1}\bar{1}0$ reflection shown in figure 1(c) the entire length of dislocation encircling the fault extinguishes at once, which is the behavior characteristic of a dislocation loop.
In the back-reflection topograph in figure 1(d), some of the axial screw dislocations are marked with **S**. While four axial screw dislocations are seen in the back-reflection topograph in figure 1(d) and in the other topographs in figure 1 to surround the dislocation loop **R**, they are physically separated from it. The origin of the dislocation loops then, since in this case the two types of defect are clearly distinct, need not be associated with the axial screw dislocations. A second dislocation loop appearing in figure 1 with the same extinction behavior as **R**, is labeled $\mathbf{R_2}$. Dislocation loop $\mathbf{R_2}$, as opposed to **R**, is involved with axial screw dislocations at either of its ends. This involvement has distorted $\mathbf{R_2}$ from the ideal rhomb of **R** where it meets these axial screw dislocations, though in its ragged ends the angles of the parallelogram are preserved. It is possible that R2 had become involved with them as it grew, a ragged end being the result of pinning by an axial screw dislocation. The partial dislocations that border triangle or parallelogram-shaped stacking faults formed during the degradation of p-n diodes fabricated on 4H-SiC wafers were determined by transmission x-ray topography to be dislocation loops of Burgers vector $\frac{1}{3}<10\bar{1}0>$, the Shockley partial type, consistent with previously reported TEM results. Some were separated from axial screw dislocations also present in the sample, indicating that the axial dislocations were not involved in the loops' nucleation; while others were seen to have interacted during their growth with the axial screw dislocations, distorting their shapes from those of ideal parallelograms.

References:

[1]. J. P. Bergman, H. Lendenmann, P. Å. Nilsson, U. Lindefelt and P. Skytt, Mater. Sci. Forum, **353-356**, *299*, 2001.

[2]. H. Lendenmann, F. Dahlquist, N. Johansson, R. Söderholm, P. Å. Nilsson, J. P. Bergman and P. Skytt, Mater. Sci. Forum, **353-356**, *727*, 2001.

[3]. J. Q. Liu, M. Skowronski, C. Hallin, R. Söderholm and H. Lendenmann, Appl. Phys. Lett., **80**, *749*, 2002.

[4]. O. Kordina, C. Hallin, R. C. Glass, A. Henry and E. Janzen, Inst. Phys. Conf. Ser., **173**, *41*, 1994.

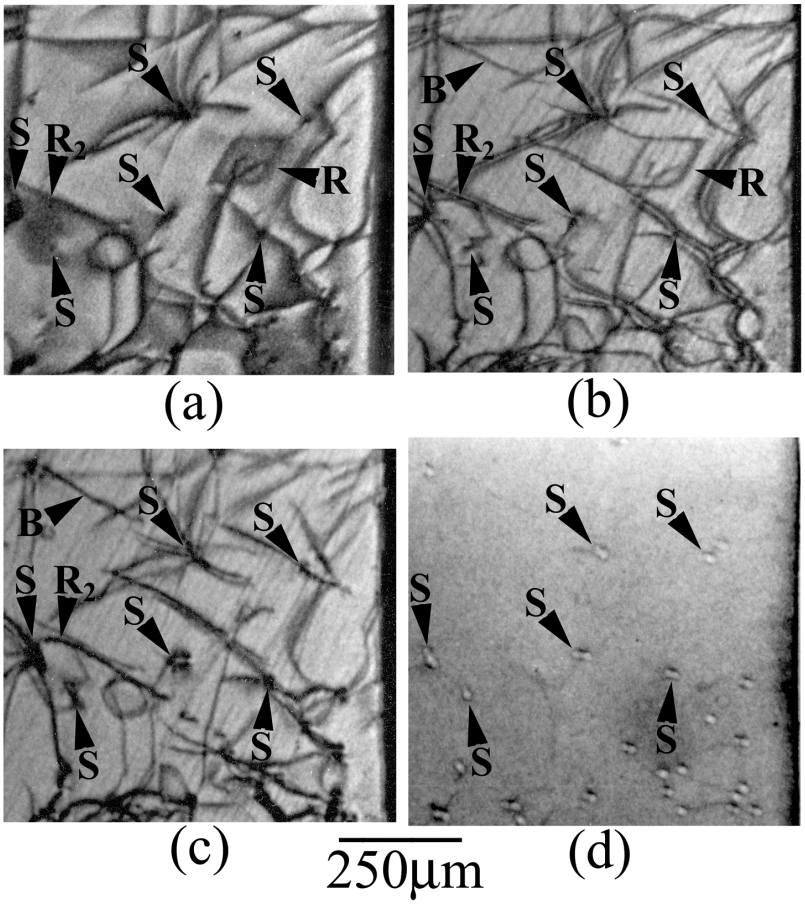

Figure 1. Synchrotron white-beam x-ray topographs of an area within a degraded diode containing polygonal dislocation loops, **R**. Also visible are basal plane dislocations, **B**, and axial screw dislocations, **S**. Transmission topographs: (a) **g** = $0\bar{1}10$, λ = 0.65 Å; (b) **g** = $11\bar{2}0$, λ = 0.59 Å; (c) **g** = $2\bar{1}\bar{1}0$, λ = 0.59 Å; back-reflection topograph: (d) **g** = 00016, λ = 1.24 Å.